Identification of Mass-Spring-Damper Model of Walking Humans

Erfan Shahabpoor[1], Aleksandar Pavic[2], Vitomir Racic[3]

[1]Research associate, INSIGNEO Institute for In-Silico Medicine, Department of Civil & Structural Engineering, University of Sheffield, UK
[2]Professor of Vibration Engineering, College of Engineering, Mathematics and Physical Sciences, University of Exeter, UK
[3]Associate Professor, Department of Civil and Environmental Engineering, Politecnico di Milano, Italy. Department of Civil & Structural Engineering, University of Sheffield, UK

Contact author: E. Shahabpoor
Department of Civil & Structural Engineering
University of Sheffield
Sir Frederick Mappin Building
Sheffield S1 3JD
E-mail: e.shahabpoor@sheffield.ac.uk
Tel: 0114-2225745
Fax: 0114-2225700

Body text word count: 5258
Number of figures: 16
Number of tables: 6

Abstract

Interaction of walking people with vibrating structures is known to be an important yet challenging phenomenon to simulate. Despite of its considerable effects on the structural response, no properly formulated and experimentally verified model currently exists to simulate this interaction in the vertical direction.

This work uses a single-degree-of-freedom mass-spring-damper model of a walking human to simulate its interaction with a vibrating structure. Extensive frequency response function measurements were performed on a test structure that was occupied by more than a hundred tests subjects walking in various group sizes and at different times in 23 tests. The identified modal properties of the occupied structure were used in three different identification procedures to estimate the parameters of the walking human model.

A discrete model of human – structure system was used to simulate interaction of each walking person with the structure. The analysis identified the range of 2.75 – 3.00 Hz for the natural frequency and 27.5 % – 30% for the damping ratio of the model of a walking human, having constant mass of 70kg. The extent of the experimental data and the measurement details, diversity of loading scenarios and consistency of the results of the different identification procedures, provided high level of confidence on the suggested parameters for the single-degree-of-freedom walking human model.

Keywords: vertical human-structure interaction; multi-pedestrian traffic; vibration serviceability; bridges; floors; moving body parameters

1 Introduction

Vibration serviceability of structures under a range of different human activities has been a growing concern to civil structural engineers since 19th century [1, 2]. The current design trends towards more slender and longer span structures have made them more susceptible than ever before to vibration serviceability problems [3, 4, 5, 6]. Investigations of several recent incidences due to walking pedestrians, both in the vertical and lateral directions, have highlighted the inability of the contemporary design guidelines to estimate reliably the vibration response [7, 8]. The key reason for this unsatisfactory situation is a widespread, yet utterly wrong, assumption that walking people affect structural dynamics only through the inertia of their moving bodies, thereby acting only as the main source of the vibration [4]. In reality, the human bodies have equally powerful effect on the modal properties of the occupied structure which, as this paper will demonstrate, should not be ignored [8, 9, 10, 11].

The simplest walking load models, such as those suggested by FIB [12], ISO 10137 [13], French design guideline [14] and UK National Annex to Eurocode 1 [15], approximate the walking force of an individual with a periodic function presentable via up to four dominant Fourier harmonics. Typically, one of these harmonics is tuned to match the frequency of a target mode of the structure to create resonance. In case of a multi-pedestrian traffic, the net force is most commonly calculated by multiplying the individual walking force by factor(s) which often depend on the pedestrian density on the structure [4, 16].

A significant move towards more realistic estimation of the structural response was made only recently by taking into account inter- and intra- subject variability of the pedestrians in the form of statistical models of their walking force [6, 17, 18, 19, 20, 21, 22]. This has increased considerably the fidelity of the walking force models, but they still cannot account fully for the human-structure interaction (HSI) [8, 11].

Mass of a stationary human body accelerates when exposed to vertical structural vibration, thereby creating an interaction force at the contact point with the structure [23]. The same applies to the moving people, in which case additional ground reaction force is created due to the self-propelling body motion. These interaction forces manifest as changes in the modal frequency of the empty structure (i.e. through the alteration of modal mass and/or stiffness) and damping. This is because such forces have components proportional to acceleration, velocity and displacement as well as independent components [24]. There have been several successful studies designed to quantify changes of the modal properties of structures when occupied by stationary (e.g. standing or sitting) people [25, 26, 27, 28, 29]. The results consistently suggested a more or less significant increase in structural damping and shifting of the natural frequency in, surprisingly, either direction. Experimental and analytical studies prompted by the Millennium Bridge problem [30] reported that walking people also add considerable damping when they excite lateral vibration modes of a structure [31]. However, similar studies on the effect of walking people on the vertical structural modes are very rare and limited [32, 33].

Zivanovic, et al. [33] did a series of FRF measurements on a test footbridge and studied the changes in the dynamic properties of the structure in the vertical direction due to the presence of either *all* standing or *all* walking groups of people. They reported a slight increase in the natural frequency and a three-fold increase of the damping of the occupied structure relative to the empty structure. Moreover, the authors observed that the walking people added less damping to the structure than the stationary people. Based on an analytical study featuring a walking human as a single-degree-of-freedom (SDOF) mass-spring-damper (MSD) oscillator, Shahabpoor, et al. [34, 35] showed that the natural frequency of a vertical mode of the occupied structure can either increase or decrease depending on the frequency of the human SDOF system, while damping of the structure always increases. These changes appeared prominent especially when the natural frequency of the human SDOF system was close to the modal frequency of the empty structure.

Miyamori, et al. [36] reported similar results using a more complex 3DOF biodynamic model of a walking individual, but also without experimental verification. Kim, et al. [37] used a simpler 2DOF MSD model with little success because the majority of the human model parameters were adapted from ISO 5982:1981 [38], which refers to stationary standing (rather than walking) people. Favored for its simplicity, the elementary SDOF MSD model was used in a number of studies to simulate pedestrian-structure interaction in the vertical direction [17, 39, 40, 41, 42, 43, 44]. However, due to the lack of knowledge about the true values of the parameters of a walking human SDOF system, the values were either assumed or adapted from sparse biomechanical studies relevant to other activities, such as bouncing and jumping. The work of Silva and Pimentel [41] and Jiménez•Alonso and Sáez [44] are the only examples to date known to the authors that proposed a range of parameters for the SDOF walking human model in the context of structural vibration serviceability. However, the suggested values were derived using the inadequate analogy with stationary people and are based on several weak assumptions, such as that the walking excitation is a single sine wave. All of these studies commonly lack verification against a sufficiently large and statistically reliable experimental walking data recorded in parallel with structural vibration response.

In recent years there have been several attempts to use biomechanical models such as the inverted pendulum (IP) model that swings in the vertical plane [45, 46, 47, 48]. Apart from the lack of adequate experimental validation, non-linear interaction mechanism which is an essential part of these models is not straightforward for implementation in design practice. Moreover, the credibility of results of IP models is usually compromised by the large number of assumptions necessary for their simulation such as the regulatory control force to maintain the steady walking gait and initial energy input.

Moving from the single walking person to multi-pedestrian walking traffic, real stochastic nature of relevant modelling parameters need to be considered. Variability of the human mass m_h, damping c_h and stiffness k_h between different people and even for the same person under different walking scenarios, interaction of people with each other and time-varying location of people on the structure, all make the human traffic-structure system highly complex. Challenges of modelling such essentially non-deterministic system have forced design guidelines to use simplistic assumptions to approximate the reality. Most of the load models, such as ISO [13], aggregate the effects of pedestrians in a walking traffic and model their net sum loading as a single force. UK National Annex to Eurocode 1 [15] and FIB [12] go further and specify "scaling factors" of the force magnitude to account for possible synchronization between pedestrians.

The works by Paulissen and Metrikine [49] and Pecol et al. [50], pertinent to the lateral direction, and by Caprani et al. [43], Silva, et al. [42] and Jiménez•Alonso and Sáez [44] pertinent to the vertical direction are very rare recent attempts to model discrete walking traffic load by simulating every individual.

In conclusion, no fully developed, well elaborated and experimentally verified model exists currently to simulate reliably enough the effects of the walking human in the *vertical* direction for a diverse range of loading scenarios and structures. This is mainly due to the challenging nature of collecting experimental data pertinent to walking people – the issue that the present study specifically aims to address.

This paper uses comprehensive measurements of pedestrian flow recorded on a laboratory-based, yet realistic, 15-tonne prototype footbridge structure. The location on the structure and speed of each pedestrian at every moment of time, their weight and the corresponding 'nominally identical' walking force on a stiff surface were recorded for all tests. Moreover, acceleration response of the structure was recorded in parallel to the walking data. A discrete traffic model was used to simulate walking people in which each individual is modeled as a SDOF MSD oscillator. By fitting the analytical Frequency Response Function (FRF) of the occupied structure to its experimental counterparts, the unknown natural frequency f_h and damping ratio ζ_h of the SDOF human oscillator were identified using three optimization methods.

Section 2 of this paper presents a brief description of two experimental campaigns and the selection of results used in this paper. In Section 3.1 the proposed identification procedures and the discrete walking traffic-structure model are described in detail. Results of the analysis are presented for two ‘stationary’ and ‘moving’ walking scenarios in Sections 3.2 and 3.3, respectively, while values of the identified parameters for each human SDOF model are determined and discussed in Section 3.4. Finally, the conclusions are presented in Section 5.

2 Experimental campaigns

Two series of tests (referred to as Series ‘A’ and ‘B’), separated by approximately a year, were carried out on the Sheffield University prototype test footbridge (Figure 1) at different times but with identical test setup. Each series comprised a set of FRF-based modal tests of the empty structure and the structure when a number of people were walking on it. In total 23 tests were carried out: 13 tests focused on the first mode and 10 tests focused on the second mode. In these tests between 2 and 15 people were walking on the structure and modal properties of the occupied structure were estimated experimentally.

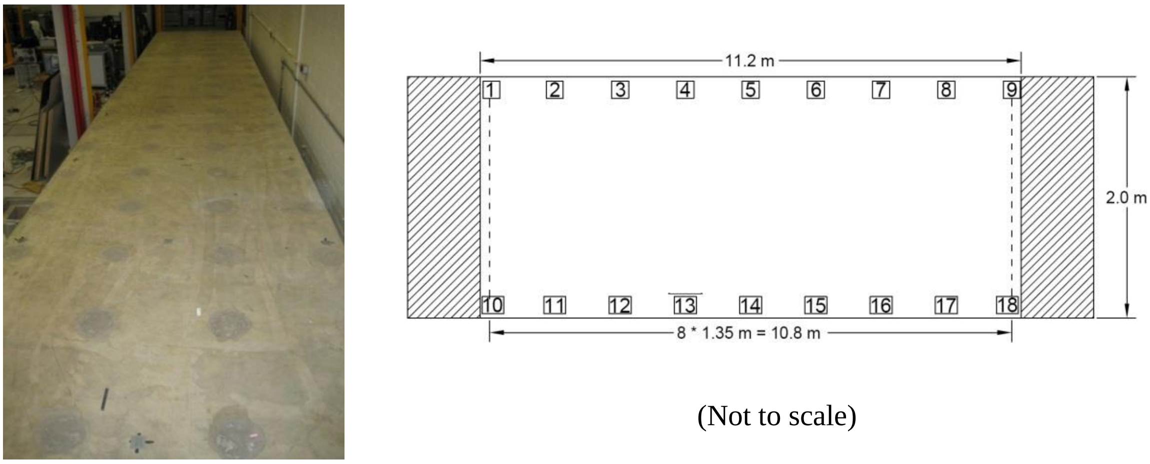

Figure 1: Photo, plan and modal test grid of the Sheffield footbridge. Two side platforms are shown with hatched rectangles.

2.1 Empty structure

The structure used in this study is a simply supported in-situ cast post-tensioned concrete footbridge purposely built in the structures laboratory of the University of Sheffield. The structure rests on two knife edge supports along its shorter edges, as illustrated in Figure 1 and behaves like a simply supported beam. The total length of the footbridge is 11.2m, including short 200 mm overhangs at the supports. Its rectangular cross section has width of 2.0 m and depth of 275 mm, and it weighs approximately 15 tonnes.

Previous modal tests of the Sheffield footbridge [11] showed that it has four modes of vibration (Figure 2) with modal frequencies less than 50 Hz. Only the first two vertical modes with modal frequencies 4.44 Hz and 16.8 Hz were considered relevant for this study. In each test series, a set of FRF-based modal testing was conducted on the empty footbridge using 18 Honeywell QA 750 accelerometers placed parallel to the longer edges of the slab (Figure 1).

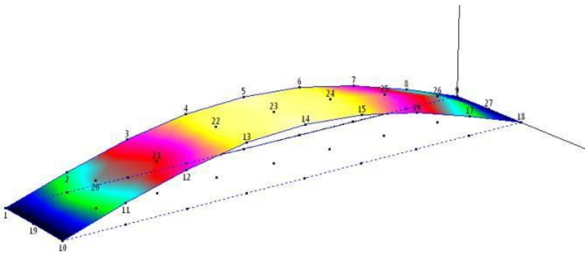

a) First vertical mode shape @ 4.44 Hz

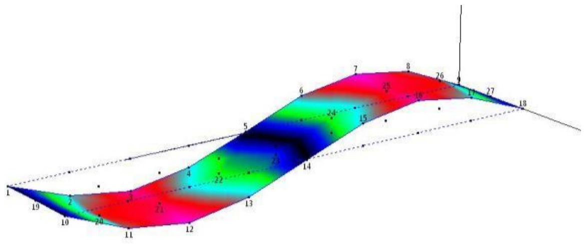

b) Second vertical mode shape @ 16.8 Hz

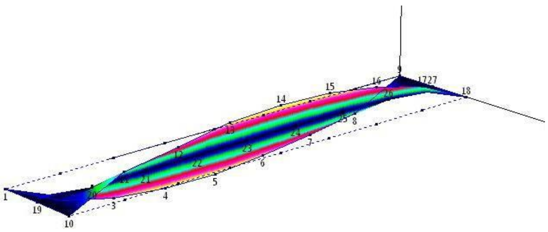

c) First torsional mode shape @25.9 Hz

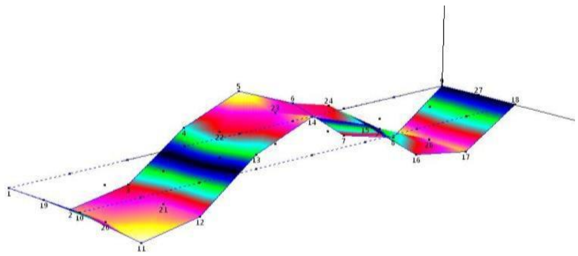

d) Third vertical mode shape @ 37.8 Hz

Figure 2: Experimentally acquired mode shapes of PT slab

In each test series A and B, two FRF-based modal tests were carried out, one for the first and one for the second mode. Chirp signals with the frequency ranges of 3.5 – 5.5 Hz for the first vertical mode (4.44 Hz), and 15 – 18 Hz range for the second vertical mode (16.8 Hz) were used to excite the structure. An APS electro-dynamic shaker model 400 [51], operated in the direct-drive mode, was connected to the slab from beneath at the mid-span or the quarter-span to get the highest possible excitation at the anti-node of the mode 1 or mode 2, respectively. The point mobility FRF was used to estimate modal properties. Empty structure modal properties are presented in Table 1 for both Series A and B tests. A slight difference between the identified modal properties of the empty structure is noticeable between Series A and B which is to be expected considering the time gap of about a year between the tests.

Table 1: Results of modal analysis of the empty structure (es)

Mode	FRF based						
#	Modal frequency f_{es}(Hz)	Modal damping ratio ζ_{es} (%)	Modal mass m_{es} (kg)	Modal damping coefficient c_{es} (N.s/m)	Modal stiffness k_{es} (N/m)	Maximum response a_{max} (m/s^2)	Response RMS a_{rms} (m/s^2)
1 (Series A)	4.44	0.6	7,128	2,386	5,547× 10^3	1.8782	0.3680
1 (Series B)	4.44	0.7	7,128	2,784	5,547× 10^3	2.6084	0.4826
2 (Series A)	16.87	0.4	7,128	6,044	80,086× 10^3	2.5080	0.4769
2 (Series B)	16.77	0.4	7,128	6,009	79,140× 10^3	3.2123	0.5942

2.2 Pedestrian data

The weight of each pedestrian was measured using a simple digital weighing scale. The walking force of each person (for their self-selected 'comfortable' walking speed) on a stiff surface was recorded using an instrumented treadmill. A pair of PeCo laser pedestrian counters [52], located 8 meters apart above the footbridge walkway (Figure 3), were used to record the time- and direction-stamped instances of each pedestrian crossing them.

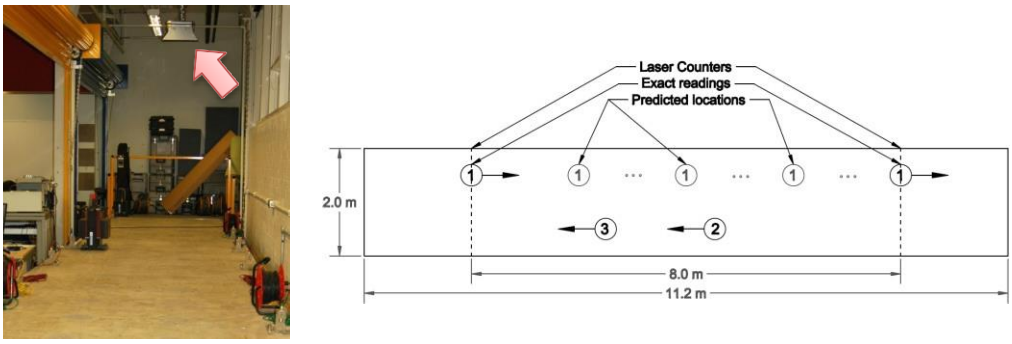

Figure 3: Prediction of people location between each two consecutive crossing of PeCo laser pedestrian counter

Figure 4 presents typical time-histories of location of three pedestrians during a 100s test. Location of each person is shown with different colour and support locations are shown with dashed lines. Time-history of each pedestrian location and walking speed were calculated by cross-comparing the PeCo data with the synchronized time-stamped video footage of each test. Walking speed was assumed constant between each two consecutive crossings of the laser counters.

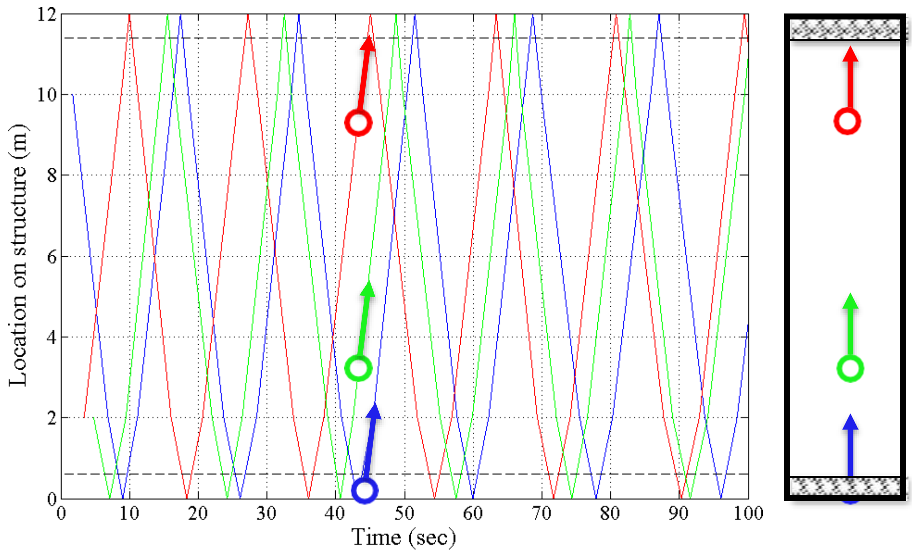

Figure 4: A typical time-history of location of three pedestrians on the structure presented with three different colors

2.3 Occupied structure tests

Two different loading scenarios were considered for this study. In the first loading scenario test participants were asked to walk around a tight circle in specific locations on the structure (mid-span, quarter-span and 3/8 span). In this loading scenario, people were assumed to be *nominally stationary* on the structure i.e. their locations on the structure were constant and assumed to be at the center of the circle (Figure 5a). This assumption is important as it eliminates the time-variance in the model of the human-structure system and makes it possible to formulate their dynamic interaction using conventional equation of motions for linear multiple-degrees-of-freedom (MDOF) systems. Eight tests, five focused on the first mode of the structure and three focused on the second mode, were carried out using this loading scenario. These tests were labeled with letter ‘C’ at the end of their test number to indicate walking in a circle (Table 2).

In the second loading scenario test participants were asked to walk in a closed-loop path along the structure (Figure 5b). Eight out of 15 tests targeted the first vertical vibration mode, while the remaining seven tests focused on the second vertical mode of vibration. Between 2 and 15 people participated in each test. They were asked to walk with their comfortable speed and were free to pass each other. 15 data blocks, each lasting 64 seconds, were acquired in each test to average out unmeasured extraneous excitation as much as possible and get better quality FRFs. The FRF test setups were identical to the empty structure tests with 18 accelerometers recording responses along the two long edges of the structure (Figure 5).

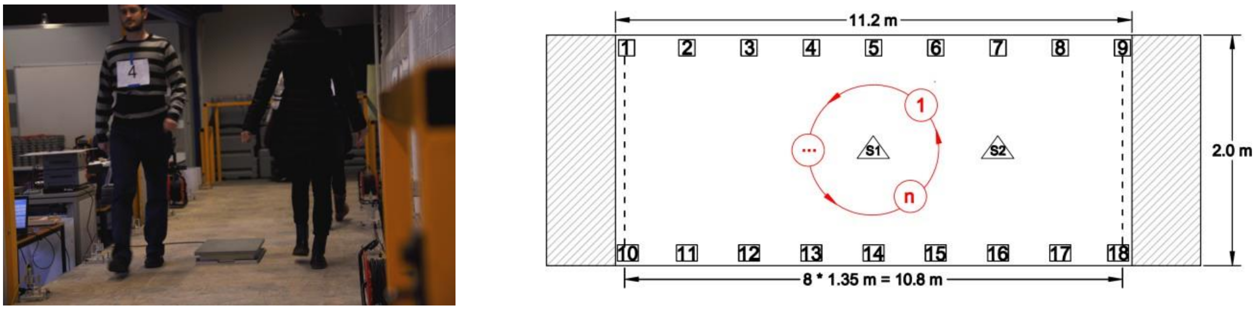

a) Scenario 1: Walking in tight circle

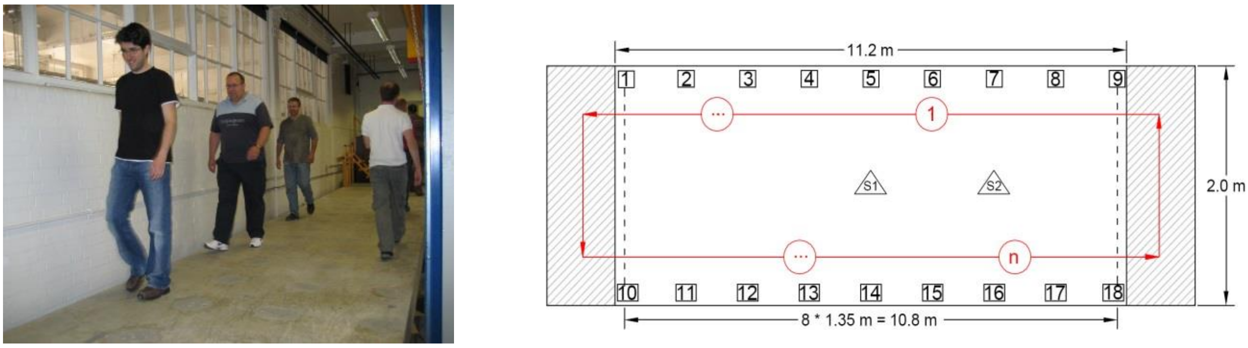

b) Scenario 2: Walking along the structure

Figure 5: A typical walking path of designed loading scenarios

Table 2: Modal properties of the occupied structure (os) for different group sizes – walking around the tight circle tests

Test No.	Series	Location	No. of Pedestrians	Modal properties of the occupied structure (os)					Structural Response	
				f_{os} (Hz)	ζ_{os} (%)	m_{os} (kg)	c_{os} (N.s/m)	k_{os} (N/m)	a_{max} (m/s^2)	a_{rms} (m/s^2)
Mode 1 (Structure)										
1.1C	B	Mid-span	3	4.455	2.00	7,214	8,077	5,652$\times 10^3$	1.3226	0.2488
1.2C	B	Mid-span	6	4.480	2.90	7,300	11,918	5,784$\times 10^3$	1.0903	0.2008
1.3C	B	Mid-span	10	4.500	3.40	7,415	14,256	5,928$\times 10^3$	0.8656	0.1861
1.4C	B	3/8 -span	6	4.465	2.50	7,287	10,222	5,735$\times 10^3$	0.9920	0.1987
1.5C	B	Quarter-span	6	4.460	2.05	7,250	83,29	5,693$\times 10^3$	1.0996	0.2195
Mode 2 (Structure)										
2.1C	B	Quarter-span	3	16.913	0.61	7,128	9,241	80,496$\times 10^3$	2.2306	0.4188
2.2C	B	Quarter-span	6	16.925	0.82	7,128	12,432	80,611$\times 10^3$	1.9406	0.3544
2.3C	B	Quarter-span	10	16.975	0.99	7,128	15,054	81,091$\times 10^3$	1.6871	0.3660

Modal parameters of the occupied structure (OS), natural frequency f_{os} [Hz], modal mass m_{os} [kg] and modal damping ratio ζ_{os} [%], were found by curve-fitting the point-mobility FRF for each test. These parameters are presented in Table 2 and Table 3 for the tight-circle (Figure 5a) and along the structure (Figure 5b) scenarios, respectively. Comparing the values of modal properties of the occupied (Table 2 and Table 3) and empty structure (Table 1), differences in the corresponding modal frequencies and particularly in damping ratios are noticeable. These changes were attributed to the effects of the HSI during walking. The identification methods developed for this paper (described in Section 0) have used these observed effects to estimate the possible properties of the human SDOF MSD model.

Table 3: Modal properties of the occupied structure (os) for different group sizes – 'walking along the structure' tests

Test No.	Series	Location	No. of Pedestrians	Modal properties of the occupied structure (os)					Structural Response	
				f_{os} (Hz)	ζ_{os} (%)	m_{os} (kg)	c_{os} (N.s/m)	k_{os} (N/m)	a_{max} (m/s^2)	a_{rms} (m/s^2)
Mode 1 (Structure)										
1.1	A	All-over	2	4.443	1.00	7,165	4,000	$5{,}583\times 10^3$	2.4361	0.4131
1.2	B	All-over	3	4.445	1.10	7,183	4,413	$5{,}603\times 10^3$	1.7489	0.3018
1.3	A	All-over	4	4.450	1.28	7,201	5,154	$5{,}630\times 10^3$	2.1755	0.3637
1.4	A	All-over	6	4.465	1.55	7,238	6,294	$5{,}696\times 10^3$	1.8771	0.3311
1.5	B	All-over	6	4.465	1.65	7,238	6,701	$5{,}696\times 10^3$	1.4882	0.2481
1.6	B	All-over	10	4.475	2.30	7,311	9,456	$5{,}780\times 10^3$	1.1313	0.2050
1.7	A	All-over	10	4.476	2.10	7,311	8,635	$5{,}782\times 10^3$	1.5876	0.2870
1.8	A	All-over	15	4.485	2.91	7,402	12,140	$5{,}878\times 10^3$	1.1251	0.2466
Mode 2 (Structure)										
2.1	B	All-over	3	16.900	0.55	7,128	8,326	$80{,}372\times 10^3$	2.4059	0.4482
2.2	A	All-over	6	16.813	0.53	7,128	7,982	$79{,}548\times 10^3$	2.9046	0.5595
2.3	B	All-over	6	16.910	0.65	7,128	9,846	$80{,}468\times 10^3$	2.2905	0.4234
2.4	A	All-over	8	16.819	0.61	7,128	9,190	$79{,}605\times 10^3$	2.5591	0.5133
2.5	A	All-over	10	16.822	0.64	7,128	9,644	$79{,}634\times 10^3$	2.5232	0.5223
2.6	B	All-over	10	16.935	0.75	7,128	11,377	$80{,}708\times 10^3$	2.1387	0.4023
2.7	A	All-over	15	16.825	0.79	7,128	11,907	$79{,}665\times 10^3$	2.2358	0.4725

2.4 Changes of mode shapes

One of the key assumptions of the identification methods used in this paper was that the presence of walking people on a structure did not affect its mode shapes. This assumption was examined by comparing the mode shapes of the empty structure and when occupied by a group of 10 (Figure 6). The acceleration responses recorded by all 18 accelerometers on the structure were used to find the first two mode shapes. The mode shape amplitudes were calculated at nine equidistant points along the central longitudinal axis of the symmetry of the footbridge. They were average values of the two mode shapes each measured at nine points along the two edges of the footbridge (eg. 10 and 1, 11 and 2, etc.). As it can be seen in Figure 6, there is no significant difference between the mode shapes of the empty and the occupied structure.

Moreover, another assumption was made that, for a given number of people walking across the structure, the modal properties of the occupied structure m_{os} [kg], c_{os} [Ns/m] and k_{os} [N/m], determined from measured FRFs, represent their *average* over the test duration. This assumption holds despite the fact that people’s location change continuously with time.

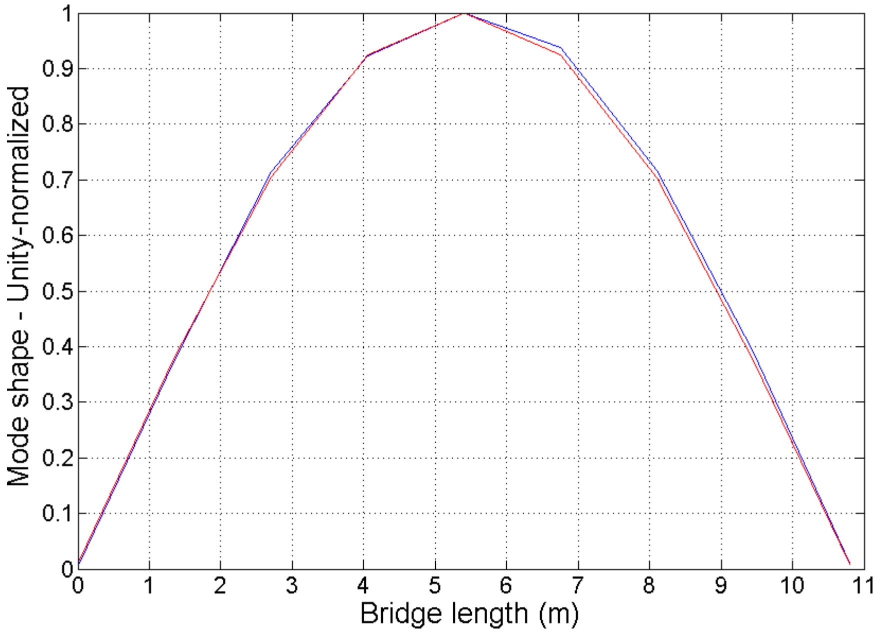

Figure 6: First mode shape of empty (blue trace) and occupied (red trace) Sheffield footbridge

3 Identification of walking human model

The core of all the identification procedures developed for this study is a ‘stationary’ walking traffic-structure model. It describes an abstract situation in which people walk on a spot, i.e. their location on the structure does not change. It can be imagined as people walking on a series of treadmills installed at fixed locations on a structure (Figure 7).

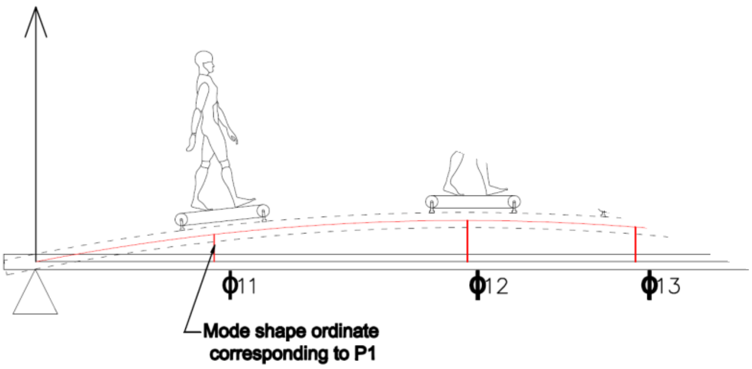

Figure 7: A conceptual illustration of stationary walking people

Figure 8 presents the MSD model of such a stationary walking traffic-structure system. The SDOF MSD model was used to simulate dynamics of each walking individual on the structure. Similarly, an SDOF model was used to simulate one mode of the structure at a time. The effects of the location of each individual on the structure were taken into account by scaling their parameters (m_h, c_h and k_h) and excitation amplitudes with the ordinate of the mode shape corresponding to their location on the structure (Φ in Figure 7 and), as appropriate in modal analysis.

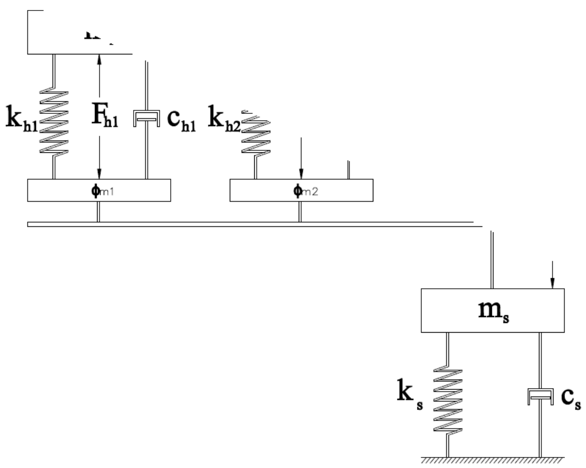

Figure 8: MDOF Mass-spring-damper model of stationary walking traffic-structure system

Being stationary, this system could be treated as a conventional MDOF system (Equation 1). A modified system of equations of motion (Equation 2) was developed that takes into account the location of people on the structure:

$$[M]\{\ddot{x}(t)\} + [C]\{\dot{x}(t)\} + [K]\{x(t)\} = \{F(t)\} \qquad \text{(Eq. 1)}$$

$$\begin{bmatrix} m_{es,j} & 0 & 0 & \cdots & 0 \\ 0 & m_{h1} & 0 & \cdots & 0 \\ 0 & 0 & m_{h2} & \cdots & 0 \\ \vdots & \vdots & \vdots & \ddots & \vdots \\ 0 & 0 & 0 & \cdots & m_{hn} \end{bmatrix} \begin{bmatrix} \ddot{x}_{os,j}(t) \\ \ddot{x}_{h1}(t) \\ \ddot{x}_{h2}(t) \\ \vdots \\ \ddot{x}_{hn}(t) \end{bmatrix} +$$

$$\begin{bmatrix} c_{es,j} + (c_{h1}\times\varphi_{1j}) + (c_{h2}\times\varphi_{2j}) + \cdots + (c_{hn}\times\varphi_{nj}) & -(c_{h1}\times\varphi_{1j}) & -(c_{h2}\times\varphi_{2j}) & \cdots & -(c_{hn}\times\varphi_{nj}) \\ -(c_{h1}\times\varphi_{1j}) & c_{h1} & 0 & \cdots & 0 \\ -(c_{h2}\times\varphi_{2j}) & 0 & c_{h2} & \cdots & 0 \\ \vdots & \vdots & \vdots & \ddots & \vdots \\ -(c_{hn}\times\varphi_{nj}) & 0 & 0 & \cdots & c_{hn} \end{bmatrix} \begin{bmatrix} \dot{x}_{os,j}(t) \\ \dot{x}_{h1}(t) \\ \dot{x}_{h2}(t) \\ \vdots \\ \dot{x}_{hn}(t) \end{bmatrix} +$$

$$\begin{bmatrix} k_{es,j} + (k_{h1}\times\varphi_{1j}) + (k_{h2}\times\varphi_{2j}) + \cdots + (k_{hn}\times\varphi_{nj}) & -(k_{h1}\times\varphi_{1j}) & -(k_{h2}\times\varphi_{2j}) & \cdots & -(k_{hn}\times\varphi_{nj}) \\ -(k_{h1}\times\varphi_{1j}) & k_{h1} & 0 & \cdots & 0 \\ -(k_{h2}\times\varphi_{2j}) & 0 & k_{h2} & \cdots & 0 \\ \vdots & \vdots & \vdots & \ddots & \vdots \\ -(k_{hn}\times\varphi_{nj}) & 0 & 0 & \cdots & k_{hn} \end{bmatrix} \begin{bmatrix} x_{os,j}(t) \\ x_{h1}(t) \\ x_{h2}(t) \\ \vdots \\ x_{hn}(t) \end{bmatrix} =$$

$$\begin{bmatrix} f_{ex,j}(t) + (f_{h1}(t)\times\varphi_{1j}) + (f_{h2}(t)\times\varphi_{2j}) + \cdots + (f_{hn}(t)\times\varphi_{nj}) \\ 0 \\ 0 \\ \vdots \\ 0 \end{bmatrix} \qquad \text{(Eq. 2)}$$

In Equation 2, $m_{es,j}$, $c_{es,j}$ and $k_{es,j}$ are mode j modal mass, damping coefficient and stiffness of the empty structure (es) and m_{hi} , c_{hi} and k_{hi} are those of the walking individuals. Viscous damping is assumed for SDOF walking human models. $\ddot{x}_{os,j}(t)$, $\dot{x}_{os,j}(t)$ and $x_{os,j}(t)$ are the acceleration, velocity and displacement response of occupied structure DOF in the system. As one mode of the structure (j) is simulated at a time, $\ddot{x}_{os,j}(t)$, $\dot{x}_{os,j}(t)$ and $x_{os,j}(t)$ also represent the *modal response* of the occupied structure. Similarly, $\ddot{x}_{hi}(t)$, $\dot{x}_{hi}(t)$ and $x_{hi}(t)$ represent acceleration, velocity and displacement of the i^{th} walking person DOF. $f_{ex,j}(t)$ is the mode ‘j’ modal force (if any) due to an external force acting on the structural DOF and $f_{hi}(t)$ is a walking force of person ‘i’ on a stiff surface. φ_{ij} is the ordinate of ‘j^{th}’ mode shape of the structure at the location of person ‘i’.

The damping matrix of the system described by Equation 2 is not necessarily proportional. Therefore, the conventional formulation of the proportionally-damped eigenvalue problem will not yield modal vectors (eigenvectors) that uncouple the equations of motion of the system [53]. The state-space technique used here to circumvent this problem involves the reformulation of the original equations of motion, for an N-degree of freedom system, into an equivalent set of 2N first order differential equations [54].

In the first step, a new coordinate vector $\{y\}$ containing displacement $x(t)$ and velocity $\dot{x}(t)$ is defined:

$$\{y(t)\} = \begin{Bmatrix} x(t) \\ \dot{x}(t) \end{Bmatrix} \qquad \text{(Eq. 3)}$$

Then Equation 2 is re-written into following form for modal analysis [54]:

$$\begin{bmatrix} [C] & [M] \\ [M] & [0] \end{bmatrix} \{y(t)\} + \begin{bmatrix} [K] & [0] \\ [0] & [-M] \end{bmatrix} \{y(t)\} = \{0\} \qquad \text{(Eq. 4)}$$

In Equation 4, [M], [C] and [K] are the mass, damping and stiffness matrices of the walking traffic-structure system, respectively, as detailed in Equation 2. Equation 4 leads to a standard eigenvalue problem and can be solved for eigenvectors and eigenvalues accordingly. Further discussion of modal analysis of systems with non-proportional damping is beyond the scope of this paper.

The MDOF system in has n+1 modes of vibration. The *dominant mode* of vibration was defined as the mode with maximum response at the ‘structure’ degree of freedom. For consistency and to allow for mode superposition, mode shapes were scaled in a way that the ordinate of the structure DOF is 1.0. Such scaling ensured that modal properties of the human-structure system are found with the same scaling as the empty structure.

3.1 Identification procedure

The identification procedure developed for this study was iterative by trial and error. Initial ranges of 1-10 Hz with 0.05 Hz steps for f_h and 5 - 70% with 2.5% steps for ζ_h were selected to model the walking human (‘h’ subscript is used here instead of ‘hi’ to refer generally to any human). These ranges were selected based on the values suggested in the biomechanics literature [36, 55, 56] and the study done by Silva, et al. [41] on walking people.

The MDOF traffic-structure model shown in was used to simulate each test and to estimate occupied structure parameters f_{os}, m_{os} and ζ_{os}. These parameters and peak FRF magnitude a_{FRF} were compared with their experimental counterparts and the corresponding errors were calculated. This process was repeated for all combinations of f_h and ζ_h for each test. The same values of f_h and ζ_h were used in each simulation for all pedestrians to reduce the number of combinations needing analysis and to make the results simpler to interpret. Mass of the human model m_h was assumed equal to the average mass of participants in the corresponding test. The values of the empty structure modal properties presented in Table 1 were used as m_{es}, k_{es} and c_{es}.

A series of maximum acceptable errors were defined for the estimated f_{os}, m_{os}, ζ_{os} and a_{FRF}. These were 0.01 Hz for f_{os}, 250 kg for m_{os}, 1% for ζ_{os} and 20% for a_{FRF}. For each test, the *ranges* of f_h and ζ_h were identified that predict f_{os}, m_{os}, ζ_{os} and a_{FRF} with errors less than the maximum acceptable. These ranges are referred to as ‘test-accepted’ ranges. In the next step, the test-accepted ranges of f_h and ζ_h were combined for all tests (each mode separately) and common ranges of f_h and ζ_h across all tests were found. This ensures that, if any combination of f_h and ζ_h (selected from these common ranges) was used to simulate people in any of the tests, the predicted f_{os}, m_{os}, ζ_{os} and a_{FRF} would be within the acceptable error ranges.

3.2 Scenario 1: Nominally 'stationary' walking traffic

Eight tests, five focused on the first mode of the structure and three focused on the second mode, were conducted using this loading scenario. The tight-circle walking pattern (Figure 5a) of this scenario is designed in a way that walking people can be assumed 'stationary' on the structure. This approximately eliminates the time-variance of the modal properties of the structure due to change of location of the people walking along the structure and makes possible to use Equation 2 without any further assumptions. As previously mentioned, the centre of the circular walking path is used as the constant location of all walking people.

Table 4 presents the test-accepted ranges of human model f_h and ζ_h resulting from this identification process. Figure 9 presents a typical set of occupied structure analytically calculated FRFs (dark grey curves) for test 1.1C (Table 4) when f_h and ζ_h were chosen from their corresponding test-accepted ranges 2.75-3.25Hz and 25-35%, respectively. As it can be seen in this figure, any combination of f_h and ζ_h selected from the corresponding test-accepted ranges (Figure 9 – dark grey FRFs) approximate occupied structure dynamics (Figure 9 – dashed blue FRF) quite well.

Table 4: Test-accepted ranges of SDOF human model parameters – Scenario 1

Test No.	No. of Pedestrians	Location	Average human mass (kg)	Acceptable ranges of SDOF human model parameters				
				f_h (Hz)		m_h (kg)	ζ_h (%)	
				Min	Max		Min	Max
Mode 1 (Structure)								
1.1C	3	Mid-span	70	2.75	3.25	70	25.0	35.0
1.2C	6	Mid-span	70	2.75	3.25	70	25.0	32.5
1.3C	10	Mid-span	70	2.25	3.00	70	25.0	30.0
1.4C	6	3/8 -span	70	2.50	3.20	70	27.5	35.0
1.5C	6	Quarter-span	70	2.50	3.40	70	27.5	40.0
Mode 2 (Structure)								
2.1C	3	Quarter-span	70	5.75	7.75	70	10.0	20.0
2.2C	6	Quarter-span	70	5.50	6.75	70	12.5	20.0
2.3C	10	Quarter-span	70	5.75	6.75	70	12.5	17.5

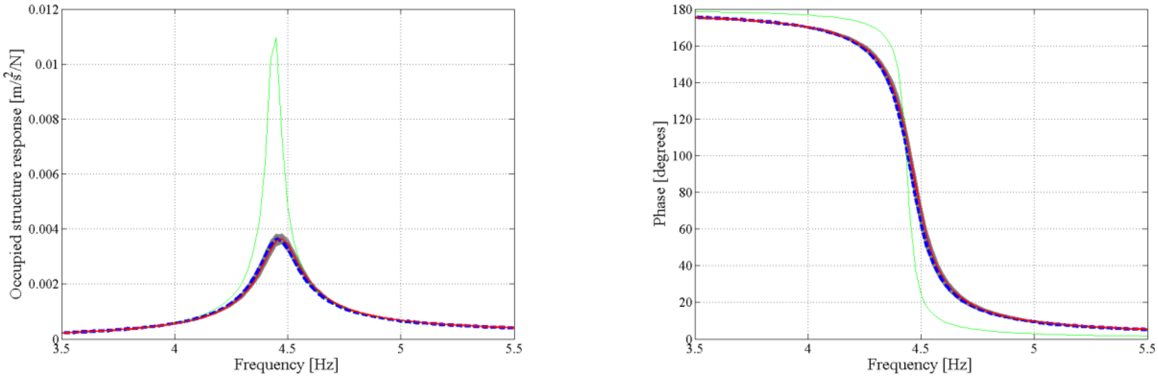

Figure 9:A typical over plot of occupied structure FRF graphs resulted from accepted human model parameters (Grey curves) – Test No 1.1C – (3 pedestrians walking at mid-span – Empty structure: green; Experimental: dashed blue; Best analytical match: red)

3.3 Scenario 2: Moving along the structure

Scenario 2 comprised 15 tests in which pedestrians were walking along the structure freely and therefore their locations on the structure changed with time. As locations of people in this scenario could not be assumed stationary, Equation 2 could not be used directly. To address this problem, two methods (Method 1 and Method 2) were developed to approximate moving people with a series of stationary cases. Using these methods made it possible to use the Equation 2 to find the occupied structure modal properties under the moving pedestrians load.

3.3.1 Method 1

Method 1 was based on the assumption that a moving traffic with constant flow of pedestrians can be simulated using a series of pre-defined location patterns and their corresponding probability of occurrence. For each test, a series of pre-defined location patterns similar to the one presented in Figure 10 was defined. These patterns were defined in a way that if pedestrians go through them repeatedly, they create a traffic flow similar to the actual traffic of the corresponding test. The structure and its two side platforms (shown in Figure 1) were divided into 9 segments of equal size. Assuming that all pedestrians were walking with an equal constant speed, the probabilities of pedestrian occurrence in each of the nine segments were equal i.e. 1/9.

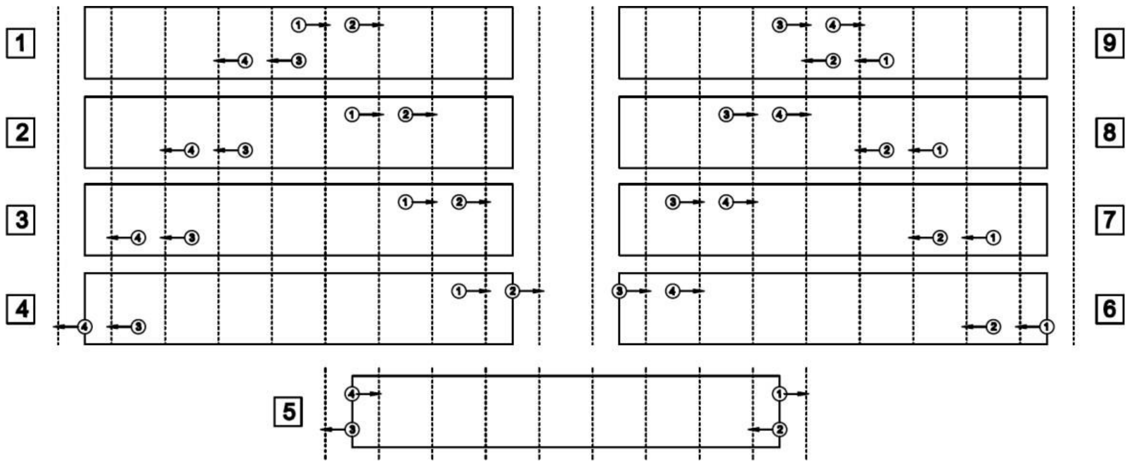

Figure 10: The illustration of pre-defined location patterns for the group of 4 pedestrians

Figure 10 shows a typical example of location patterns for a group of four people walking on the test footbridge. Nine location patterns with equal probability of occurrence were defined for this walking group, among which, the pairs of patterns 1 and 9, 2 and 8, 3 and 7, and 4 and 6 create the same dynamic effect on the structure. This is because the mode 1 shape is symmetric and the mode 2 shape is anti-symmetric with respect to the mid-span point. Therefore, 5 unique location patterns with the following probabilities were considered for this test:

- Pattern 1 (or 9) - Probability: 2/9
- Pattern 2 (or 8) - Probability: 2/9
- Pattern 3 (or 7) - Probability: 2/9
- Pattern 4 (or 6) - Probability: 2/9
- Pattern 5: - Probability: 1/9

For each location pattern, pedestrians were assumed stationary and Equation 2 was used to simulate the stationary traffic-structure system. The resulting occupied structure modal properties f_{os} and ζ_{os} (and resulting FRF), were then averaged for all location patterns based on their probability of occurrence. The resulting average FRF found for the structure in each simulation was assumed to represent the occupied structure FRF. These FRFs were later compared with their experimental counterpart to find the test-accepted ranges of human model f_h and ζ_h.

Figure 11 shows a typical over plot of the occupied structure FRFs for five pre-defined location patterns (grey curves) and the average FRF (red) corresponding to test 1.2 (Table 5). The good match between the average analytical and experimental FRF curves (dashed blue) can be seen in this figure.

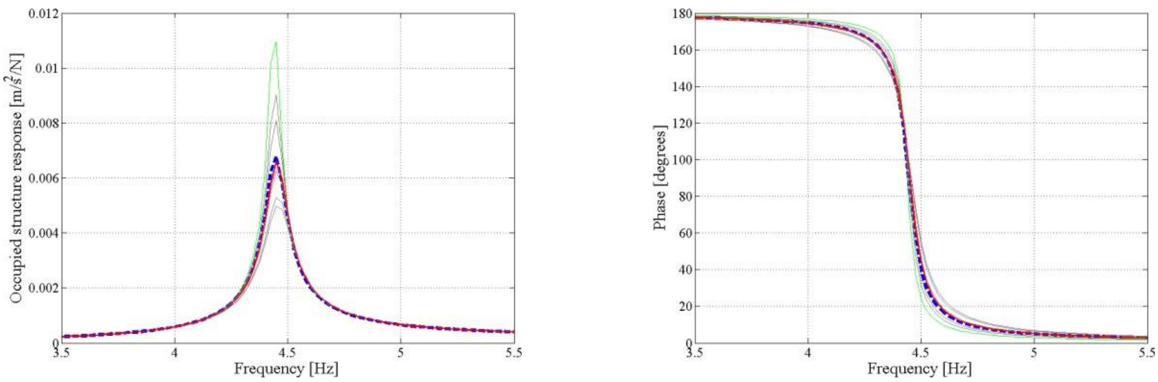

Figure 11: A typical over plot of occupied structure FRF graphs for different location patterns and the average FRF– Test 1.2 – (Empty structure: Green; Curves corresponding to different patterns: grey; Average analytical: red; Experimental: dashed blue)

The test-accepted ranges of human model f_h and ζ_h resulting from simulations are presented in Table 5. The over-plot of average occupied structure FRFs for test-accepted f_h and ζ_h (2.5Hz < f_h < 3.0Hz and 25% < ζ_h < 40%) corresponding to test 1.2 is presented in Figure 12. As it can be seen, similar to Scenario 1, any combination of f_h and ζ_h selected from the corresponding test-accepted ranges (dark grey FRFs – 77 combinations, i.e. FRFs, in total) approximate the occupied structure dynamics (dashed blue FRF) quite well.

Table 5: Test-accepted ranges of SDOF human model parameters – Scenario 2- Method 1

Test No.	No. of Pedestrians	Location	Average human mass (kg)	Acceptable ranges of SDOF human model parameters				
				f_h (Hz)		m_h (kg)	ζ_h (%)	
				Min	Max		Min	Max
Mode 1 (Structure)								
1.1	2	All-over	55	2.50	3.50	55	22.5	40.0
1.2	3	All-over	70	2.50	3.00	70	25.0	40.0
1.3	4	All-over	55	2.25	3.50	55	22.5	37.5
1.4	6	All-over	55	2.50	3.25	55	20.0	30.0
1.5	6	All-over	70	2.50	3.25	70	22.5	32.5
1.6	10	All-over	70	2.50	3.25	70	27.5	32.5
1.7	10	All-over	60	2.75	3.25	60	22.5	32.5
1.8	15	All-over	70	2.50	3.00	70	27.5	32.5
Mode 2 (Structure)								
2.1	3	All-over	80	6.50	8.00	80	10.0	20.0
2.2	6	All-over	55	6.50	7.25	55	10.0	17.5
2.3	6	All-over	70	5.75	7.00	70	10.0	20.0
2.4	8	All-over	75	5.50	6.75	75	10.0	17.5
2.5	10	All-over	55	6.00	7.00	55	10.0	17.5
2.6	10	All-over	70	5.75	6.75	70	10.0	20.0
2.7	15	All-over	70	5.00	6.75	70	10.0	17.5

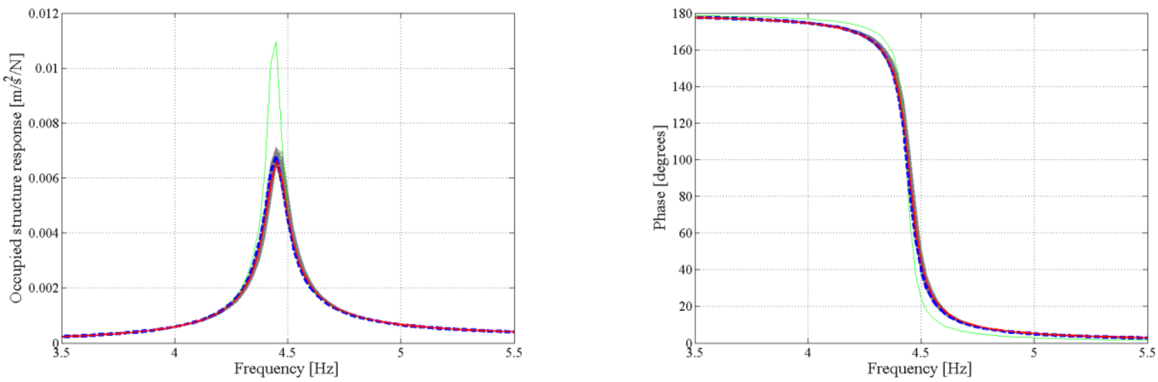

Figure 12: A typical over plot of average occupied structure FRF graphs resulted from accepted human model parameters (Grey curves) – Test 1.2– (Empty structure: green; Average analytical: red; Experimental: dashed blue)

3.3.2 Method 2

The second method takes the procedure of location simulation one step forward and uses the instantaneous location of each person recorded during each test. For each time-step, location of each pedestrian on the structure was read from the corresponding recorded location time-histories (Figure 4). The walking people were assumed stationary at their locations for that time-step and stationary traffic-structure model (Equation 2) was used to find the occupied structure modal properties for that particular time-step. This kind of simulation was repeated for all time-steps of each test. Using this procedure, time-histories of the change of the occupied structure modal parameters $f_{os}(t)$, $\zeta_{os}(t)$ and $m_{os}(t)$ for each test were found. A typical time-history of $f_{os}(t)$ and $\zeta_{os}(t)$ resulting from a random pair of test-accepted f_h and ζ_h corresponding to test 1.2 is presented in Figure 13.

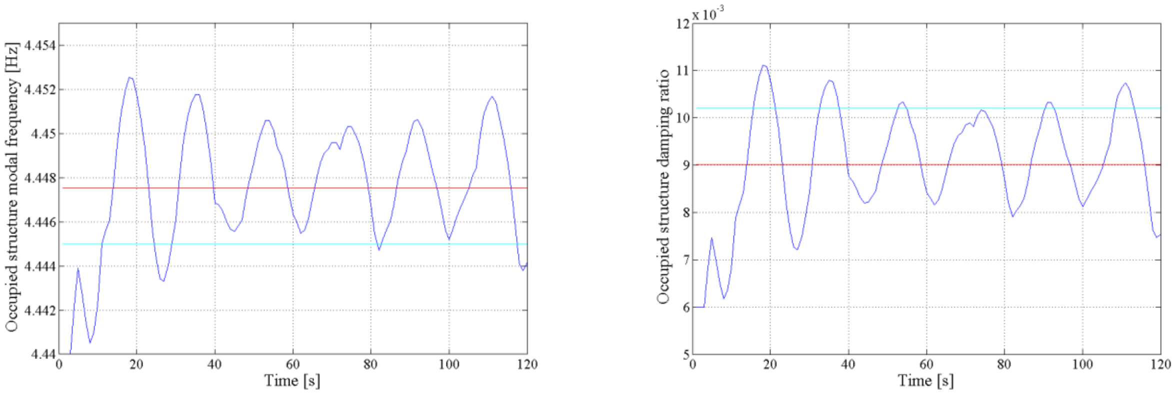

Figure 13: A typical time-history of f_{os} and ζ_{os} (blue), average value(red) and experimental value (cyan) resulted from a typical accepted human model parameter set – Test No 1.2 – (3 pedestrians)

The $f_{os}(t)$ and $\zeta_{os}(t)$ were then averaged for each test over time and the averaged parameters (and the corresponding FRF) were assumed to represent the dynamics of the occupied structure. These FRFs were later compared to their experimental counterpart to find the test-accepted ranges of human model f_h and ζ_h.

The test-accepted ranges of SDOF human model parameters f_h and ζ_h found in these simulations are presented in Table 6. The over plotted occupied structure FRFs corresponding to the test-accepted f_h and ζ_h (in test 1.2) are presented in Figure 14. As it can be seen, similar to the results of Method 1, any combination of f_h and ζ_h selected from the corresponding test-accepted ranges approximated the occupied structure dynamics quite accurately.

Table 6: Test-accepted ranges of SDOF human model parameters – Scenario 2: Method 2

Test No.	No. of Pedestrians	Location	Average human mass (kg)	Acceptable ranges of SDOF human model parameters: f_h (Hz) Min	f_h (Hz) Max	m_h (kg)	ζ_h(%) Min	ζ_h(%) Max
Mode 1 (Structure)								
1.1	2	All-over	55	2.50	3.50	55	20.0	40.0
1.2	3	All-over	70	2.25	3.25	70	20.0	40.0
1.3	4	All-over	55	2.25	3.25	55	25.0	37.5
1.4	6	All-over	55	2.50	3.25	55	20.0	30.0
1.5	6	All-over	70	2.25	3.00	70	22.5	32.5
1.6	10	All-over	70	2.50	3.00	70	25.0	32.5
1.7	10	All-over	60	2.75	3.00	60	22.5	30.0
1.8	15	All-over	70	2.25	3.00	70	27.5	32.5
Mode 2 (Structure)								
2.1	3	All-over	80	6.50	7.75	80	10.0	17.5
2.2	6	All-over	55	6.50	7.50	55	10.0	17.5
2.3	6	All-over	70	6.00	6.75	70	10.0	20.0
2.5*	10	All-over	55	6.00	7.00	55	10.0	17.5
2.6	10	All-over	70	6.00	6.75	70	10.0	17.5

* 2.4 and 2.7 are not analyzed as location time history was not available.

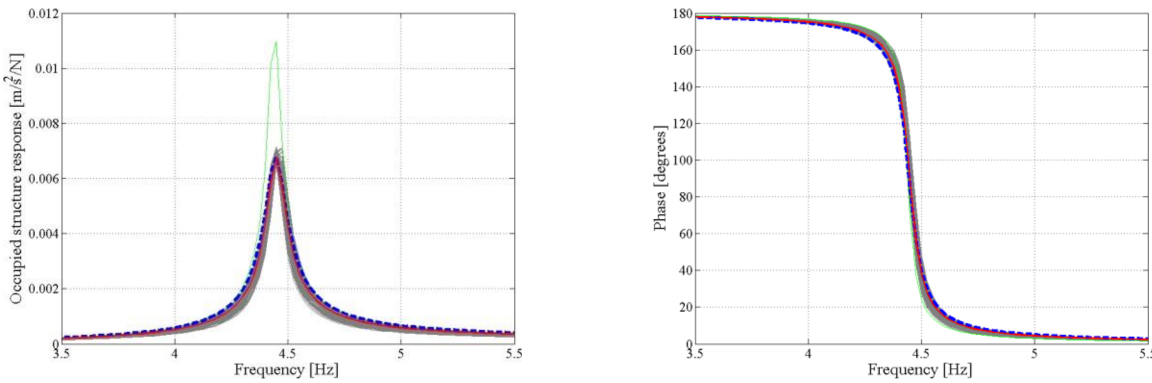

Figure 14: A typical over plot of empty (green), test-accepted occupied structure FRF graphs (grey), analytical average FRF (red) and experimental FRF (blue) resulted from test-accepted human model parameters – Test 1.2 – (3 pedestrians)

3.4 Common ranges of human model parameters

The test-accepted ranges found in all simulations of both scenarios were compared and a common range was found for f_h and ζ_h for each of the two modes. For the tests targeting the first mode of the test structure, these common ranges (between the pink and green lines, as shown in Figure 15) were found to be 2.75 – 3.00 Hz for f_h and 27.5 % – 30% for ζ_h. These ranges were found to be 6.5 – 6.75 Hz and 12.5 % – 17.5% respectively for the tests targeting the second mode of the structure.

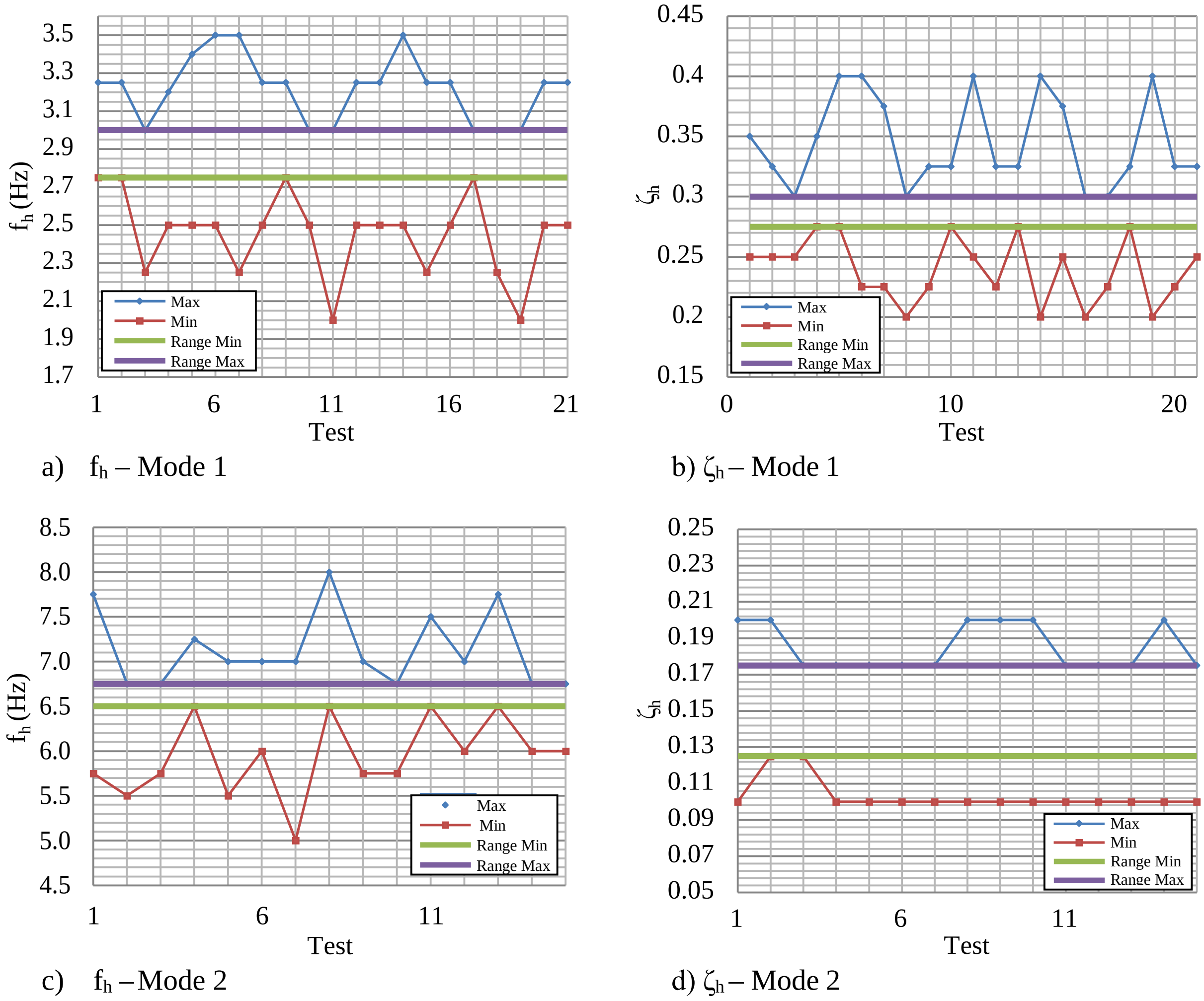

Figure 15: Test-accepted ranges of f_h and ζ_h found in different tests and their common ranges

3.5 Expected errors

To understand how good each arbitrary combination of f_h and ζ_h selected from their common ranges (across all tests) can predict the occupied structure dynamics, simulations were repeated for all mode 1 tests but this time with common ranges of f_h and ζ_h as input. The occupied structure parameters f_{os}, ζ_{os} and a_{FRF} were estimated for each combination of f_h and ζ_h and compared with their corresponding experimental values to find the associated errors. The absolute errors associated with the estimated f_{os}, ζ_{os} and a_{FRF} for each combination of f_h and ζ_h were averaged over all tests and presented in Figure 16. As it can be seen in these graphs, the minimum errors of estimating f_{os}, ζ_{os} and a_{FRF} were not associated with a unique set of f_h and ζ_h i.e. no particular set of f_h and ζ_h can predict all f_{os}, ζ_{os} and a_{FRF} with minimum error at the same time. However, for engineering purposes, it is clear that errors are so small that any combination of the f_h and ζ_h from the identified common ranges would yield good approximation of the occupied structure modal properties for any number of up to 15 pedestrians.

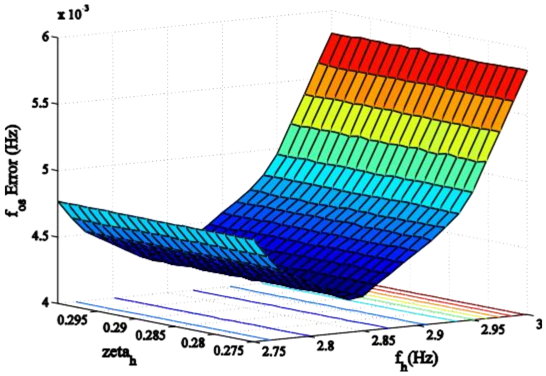

a) f_{os} Error

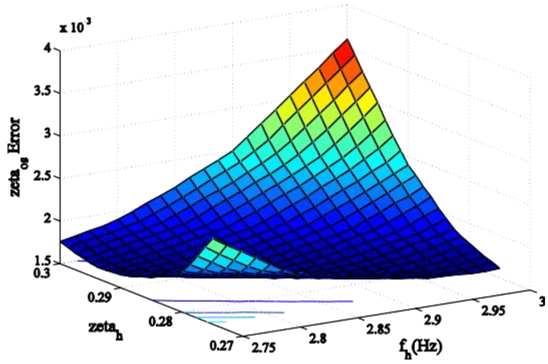

b) ζ_{os} Error

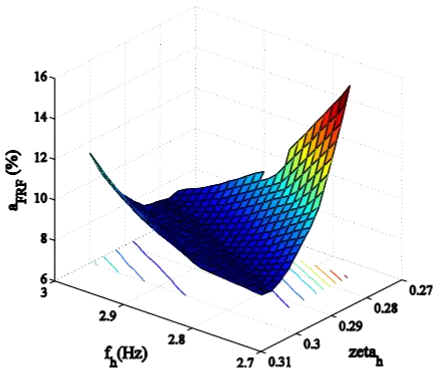

c) a_{FRF} Error

Figure 16: Expected errors in occupied structure natural frequency f_{os}, damping ratio ζ_{os} and peak FRF magnitude a_{FRF} for the common ranges of human model parameters –Mode 1

4 Comparison with other published findings

The works of Silva and Pimentel [41] and Jiménez•Alonso and Sáez [44] are the only examples to date known to the authors that specifically investigated parameters for the SDOF walking human model in the context of structural vibration serviceability. Silva and Pimentel [41] identified the parameters of an SDOF MSD walking human model by analyzing the correlation of the walking force and the acceleration of the human body recorded at waist. Assuming human mass equal to 70kg and 1.8Hz mean pacing frequency, their model suggests f_h=2.64Hz and ζ_h = 0.55 for an SDOF walking human model.

Jiménez•Alonso and Sáez [44] used a 3DoFs model, comprised of three independent SDOF MSD to simulate interaction of a walking human with a structure in each direction. They used the experimental data reported by Georgakis and Jorgesen [57] in an inverse dynamics procedure to identify the parameters of the SDOF human model in the vertical direction by trial and error. Their study suggested that an SDOF MSD model with a mass equal to 84% of the total body mass, damping ratio of 47% and natural frequency of 2.75Hz can simulate dynamic effects of a walking human on structures in the vertical direction.

The walking human model parameters suggested by both studies are comparable with the findings of this research for the first vertical mode of structure although the damping ratios proposed are slightly higher than what is presented in this paper..

Findings of this research are also in line with the findings of Shahabpoor et al. [34]. Based on an analytical study of 2DOF MSD model of a crowd-structure system, they suggested that when the natural frequency of the occupied structure f_{os} is higher than that of the empty structure fes, the natural frequency of the human/crowd model f_h is lower than the natural frequency of the empty structure $f_h<f_{es}$.

5 Conclusions

The work presented in this paper used a comprehensive and unique set of human traffic-structure experimental data to identify the parameters of the SDOF walking human model. Three different identification processes were applied with increasing level of detail for simulating the effects of location of each individual as they walk on the structure. The analysis of effects of HSI on the fundamental vertical mode of the structure yielded the ranges of 2.75 – 3.00Hz and 27.5% – 30% for the natural frequency and damping ratio of the SDOF MSD walking human model, respectively. These ranges were found to be 6.5 – 6.75 Hz and 12.5 % – 17.5% respectively for the tests targeting the second vertical mode of the structure, indicating likely presence of the higher mode of the human body which got engaged more within the frequency range of the second mode of the structure. The measured average mass of people of 70 kg was used as the SDOF mass of the walking human model. The different *walking* human model parameters found for the first two vertical vibration modes of the structure is the key novel finding and can be an indicator of MDOF nature of walking human model.

These results compare reasonably well with independently proposed values reported in the only directly relevant works to date done by Silva, et al. [41] and Jiménez•Alonso and Sáez [44]. The comprehensive experimental data, variety of loading scenarios, detailed simulation process and coherent results from different methods provide high level of confidence about the validity of the findings.

The experimental data set used in this research can serve as a benchmark for data collection for future multi-pedestrian HSI studies. Moreover, the proposed methodologies for simulating time-varying location of the walking people on the structure proved to be accurate and practically applicable, so they can be used by design engineers to simulate the walking traffic.

Further research on different real-life structures is needed using the proposed methodology to extend and validate the findings of this research for different structures and loading scenarios.

Acknowledgements

The authors acknowledge the financial support which came from the UK Engineering and Physical Sciences Research Council (EPSRC) for Platform Grant EP/G061130/2 (Dynamic Performance of Large Civil Engineering Structures: An Integrated Approach to Management, Design and Assessment) and EP/I029567/1 (Synchronization in dynamic loading due to multiple pedestrians and occupants of vibration-sensitive structures).

References

[1] Tredgold, T., 1828. Elementary principles of carpentry. 2nd edition.

[2] Figueiredo, F.P., da Silva, J.G.S., de Lima, L.R.O., da S. Vellasco, P.C.G. and de Andrade, S.A.L., 2008. A parametric study of composite footbridges under pedestrian walking loads. Engineering Structures, 30, pp.605–615.

[3] Živanović, S., Pavic, A. and Reynolds, P., 2005. Vibration serviceability of footbridges under human-induced excitation: a literature review. Journal of Sound and Vibration, 279(1–2), pp.1-74. ISSN 0022-460X.

http://dx.doi.org/10.1016/j.jsv.2004.01.019.

[4] Racic, V., Pavic, A., and Brownjohn, J.M.W., 2009. Experimental identification and analytical modelling of human walking forces: Literature review. Journal of Sound Vibration, 326(1–2), pp.1–49.

[5] Ingólfsson, E.T., Georgakis, C.T., Ricciardelli, F., and Jönsson, J., 2012. Experimental identification of pedestrian-induced lateral forces on footbridges. Journal of Sound and Vibration, 330(6), pp.1265–1284.

[6] Caprani, C.C., 2014. Application of the pseudo-excitation method to assessment of walking variability on footbridge vibration. Computers and Structures, 132, pp. 43–54.

[7] Pimentel, R.L., Pavic, A., and Waldron, P. 2001. Evaluation of design requirements for footbridges excited by vertical forces from walking. Canadian Journal of Civil Engineering, 28(5), pp.769–777. doi:10.1139/l01-036.

[8] Živanović, S., Pavic, A. and Ingolfsson, E.T., 2010. Modelling spatially unrestricted pedestrian traffic on footbridges. Journal of Structural Engineering, 136 (10), pp.1296 – 1308.

[9] Brownjohn, J.M.W., Fok, P., Roche, M. and Omenzetter, P., 2004. Long span steel pedestrian bridge at Singapore Changi Airport—part 2: crowd loading tests and vibration mitigation measures. Structural Engineer, 82 (16), pp.28–34.

[10] Kasperski, M., Sahnaci C., 2007. Serviceability of pedestrian structures. Proceedings of the 25^{th} international modal analysis conference, Orlando, Florida. pp.774–98.

[11] Shahabpoor, E., Pavić, A., 2012. Comparative evaluation of current pedestrian traffic models on structures. Conference Proceedings of the Society for Experimental Mechanics Series, 26, pp 41-52.

[12] The International Federation for Structural Concrete (FIB), 2005. Guidelines for the design of footbridges.

[13] International Organization for Standardization (ISO), 2007. Bases for design of structures: Serviceability of buildings and walkways against vibrations. ISO 10137:2007, Geneva.

[14] Technical Department for Transport, Roads and Bridges Engineering and Road Safety/French Association of Civil Engineering (SETRA/AFGC), 2006. Footbridges: Assessment of vibrational behavior of footbridges under pedestrian loading. Technical Guide 0611, Paris.

[15] British Standards Institution (BSI), 2008. UK national annex to Eurocode 1: Actions on structures. Part 2: Traffic loads on bridges, NA to BS EN 1991-2:2003 London.

[16] Ingólfsson, E.T., Georgakis, C.T., and Svendsen, M.N. 2008. Vertical footbridge vibrations: Details regarding and experimental validation of the response spectrum methodology. Proceeding of Footbridge conference.

[17] Brownjohn, J.M.W., Pavic, A. and Omenzetter, P.A., 2004. Spectral density approach for modeling continuous vertical forces on pedestrian structures due to walking. Canadian Journal of Civil Engineering, 31(1), pp.65–77.

[18] Racic, V. and Brownjohn, J.M.W., 2011. Stochastic model of near-periodic vertical loads due to humans walking. Advanced Engineering Informatics, 25, pp.259–75.

[19] Živanović, S., Pavic, A. and Reynolds, P., 2007. Probability-based prediction of multi-mode vibration response to walking excitation. Engineering Structures, 29(6), pp.942–54.

[20] Živanović, S. and Pavic, A., 2009. Probabilistic modelling of walking excitation for building floors. Journal of Performance of Constructed Facilities, 23(3), pp.132 – 143.

[21] Piccardo, G. and Tubino, F., 2012. Equivalent spectral model and maximum dynamic response for the serviceability analysis of footbridges. Engineering Structures, 40(7), pp.445–56.

[22] Krenk, S., 2012. Dynamic response to pedestrian loads with statistical frequency distribution. ASCE Journal of Engineering Mechanics, 138(10), pp.1275–81.

[23] Griffin, M.J., 1990. Handbook of human vibration, Academic Press, London.

[24] Racic, V., Brownjohn, J.M.W., Pavic, A., 2010. Reproduction and application of human bouncing and jumping forces from visual marker data. Journal of Sound and Vibration, 329, pp.3397-3416.

[25] Sachse, R., Pavic, A. and Reynolds, P., 2002. The Influence of a Group of Human Occupants on Modal Properties of a Prototype Assembly Structure. Proceeding of the 5th European Conference on Dynamics EURODYN, pp.1241-1246.

[26] Sachse, R., Pavic, A. and Reynolds, P., 2003. Human-structure dynamic interaction in civil engineering dynamics: A literature review. The Shock and Vibration Digest, 35(1), pp.3-18. ISSN 0583-1024.

[27] Butz, C., Feldmann, M. and Heinemeyer, C., 2008. Advanced load models for synchronous pedestrian excitation and optimized design guidelines for steel footbridges. RFSRCT- 2003-00019, European Commission, Brussels, Belgium.

[28] Reynolds, P., Pavic, A. and Ibrahim, Z., 2004. Changes of Modal properties of a stadium structure occupied by a crowd. Proceeding of the 22nd International Modal Analysis Conference (IMAC XXII).

[29] Salyards, K. and Firman, R., 2011. Human-structure interaction effects of crowd characteristics. Conference Proceedings of the Society for Experimental Mechanics Series, Civil Engineering Topics, 4, pp.247-254.

[30] Fitzpatrick, A., Dallard, P., le Bourva, S., Low, A., Ridsill Smith, R. and Willford, M., 2001. Linking London: The Millennium Bridge. The Royal Academy of Engineering, London.

[31] Bocian, M., Macdonald, J., and Burn, J., 2012. Biomechanically inspired modelling of pedestrian-induced forces on laterally oscillating structures. Journal of Sound and Vibration, 331, pp.3914–3929. http://dx.doi.org/10.1016/j.jsv.2012.03.023

[32] Barker, C., and Mackenzie, D., 2008. Calibration of the UK National Annex. The Proceedings of the Third Footbridge International Conference, Porto, Portugal.

[33] Živanović, S., Diaz, I.M. and Pavić, A., 2009. Influence of walking and standing crowds on structural dynamic properties. Proceeding of Conference & Exposition on Structural Dynamics (IMAC XXVII).

[34] Shahabpoor, E., Pavić, A. & Racic, V., 2013. Using MSD Model to Simulate Human-Structure Interaction during Walking. Conference Proceedings of the Society for Experimental Mechanics Series.

[35] Shahabpoor, E., Pavić, A. & Racic, V., 2013. Sensitivity Analysis of Coupled Crowd-structure System dynamics to Walking Crowd Properties. Conference Proceedings of the 5th International Conference on Structural Engineering, Mechanics and Computation (SEMC 2013).

[36] Miyamori, Y., Obata, T., Hayashikawa, T., Sato, K., 2001. Study on identification of human walking model based on dynamic response characteristics of pedestrian bridges, in: Proceedings of the Eighth East Asia-Pacific Conference on Structural Engineering & Construction (EASEC-8), Singapore.

[37] Kim, S.H., Cho, K.I., Choi, M.S., and Lim, J.Y. 2008. Development of human body model for the dynamic analysis of footbridges under pedestrian induced excitation. International Journal of Steel Structures, 8(4), pp.333–345.

[38] International Organization for Standardization (ISO), 1981. Mechanical driving point impedance of the human body. ISO 5982:1981.

[39] Archbold, P.j., 2004. Interactive load models for pedestrian footbridges. PhD Thesis, University College Dublin.

[40] Archbold, P.J., Keogh, J., Caprani, C., and Fanning. P., 2011. A Parametric Study of Pedestrian Vertical Force Models for Dynamic Analysis of Footbridges. Proceeding

of Experimental Vibration Analysis for Civil Engineering Structures Conference (EVACES 2011).

[41] Silva, F.T., and Pimentel, R.L., 2011. Biodynamic walking model for vibration serviceability of footbridges in vertical direction. Proceeding of the 8th International Conference on Structural Dynamics (Eurodyn 2011), pp.1090–1096.

[42] Silva, F.T. Brito, H.M. and Pimentel. R.L., 2013. Modeling of crowd load in vertical direction using biodynamic model for pedestrians crossing footbridges. Canadian Journal of Civil Engineering, 40, pp.1196–1204.

http://dx.doi.org/10.1139/cjce-2011-0587

[43] Caprani, C.C., Keogh, J., Archbold, P., and Fanning, P., 2011. Characteristic vertical response of a footbridge due to crowd loading. Proceeding of the 8th International Conference on Structural Dynamics (Eurodyn 2011), pp.978–985.

[44] Jiménez Alonso, J.F., Sáez, A., 2014. A direct pedestrian-structure interaction model to characterize the human induced vibrations on slender footbridges. Informes de la Construcción, 66 (EXTRA1):m007, doi: http://dx.doi.org/10.3989/ic.13.110.

[45] Qin, J.W., Law, S.S., Yang, Q.S. and Yang, N., 2013. Pedestrian–bridge dynamic interaction, including human participation. Journal of Sound and Vibration, 332(4), pp.1107-1124, ISSN 0022-460X, http://dx.doi.org/10.1016/j.jsv.2012.09.021.

[46] Qin, J.W., Law, S.S., Yang, Q.S. and Yang, N., 2014. Finite Element Analysis of Pedestrian-Bridge Dynamic Interaction. Journal of Applied Mechanics, 81(4), DOI: 10.1115/1.4024991.

[47] Bocian, M., Macdonald, J., and Burn, J. 2011. Modelling of self-excited vertical forces on structures due to walking pedestrians. Proceedings of the 8th International Conference on Structural Dynamics (EURODYN 2011) ISBN 978-90-760-1931-4.

[48] Bocian, M., Macdonald, J., and Burn, J. 2013. Biomechanically Inspired Modeling of Pedestrian-Induced Vertical Self-Excited Forces. Journal of Bridge Engineering 18, pp.1336–1346.

[49] Paulissen, J.H. and Metrikine. A.V., 2011. Non-linear dynamic modelling of adaptive pedestrian behavior on lively footbridges. Proceedings of the 8th International Conference on Structural Dynamics (EURODYN 2011).

[50] Pecol, P., Dal Pont, S., Silvano, E., Joanna, B. and Argoul, P., 2011. A 2D discrete model for crowd-structure interaction. Proceeding of the 4th Footbridges international conference.

[51] APS Dynamics, 2014. APS 400 ELECTRO-SEIS Long Stroke Shaker with Linear Ball Bearings. Available at:

http://www.apsdynamics.com/images/stories/Prospekte/APS_Shaker/APS_400/APS_400_Data_Sheet_en.pdf [Accessed 10 June 2015].

[52] SICK Sensor Intelligence, 2009. LD-PeCo People Counter: Operating instructions. Available at: https://www.sick.com/media/pdf/7/47/247/IM0011247.PDF. Last accessed: 10 June 2015.

[53] Clough, W. and Penzien, J., 1993. Dynamics of structures. 2nd edition, McGraw-Hill, New York. ISBN 0-07-011394-7.

[54] Frazer, R.A., Duncan, W.J. and Collar, A.R., 1957. Elementary Matrices. Cambridge University Press.

[55] Sachse, R., Pavic, A. and Reynolds, P., 2004. Parametric study of modal properties of damped two-degree-of-freedom crowd–structure dynamic systems. Journal of Sound and Vibration, 274, pp. 461–480.

[56] Ferris, D. P., Louie, M. and Farley, C. T., 1998. Running in the real world: adjusting leg stiffness for different surfaces. Proceeding of the Royal Society, London, 265, pp. 989-994.

[57] Georgakis, C.T. and Jorgensen, N.G., 2013. Change in mass and damping on vertically vibrating footbridges due to pedestrians. Proceedings of the 31st Conference on Structural Dynamics (IMAC 2013) 3(4), pp.37-45.